

# A method to Quantify the Affinity of Cabazitaxel for PLA-PEG Nanoparticles and Investigate the Influence of the Nano-Assembly Structure on the Drug/Particle Association

O. Diou<sup>1</sup> · S. Greco<sup>1</sup> · T. Beltran<sup>1</sup> · D. Lairez<sup>2</sup> · J.-R. Authelin<sup>1</sup> · D. Bazile<sup>1</sup>

Received: 10 February 2015 / Accepted: 9 April 2015 / Published online: 22 April 2015  
© Springer Science+Business Media New York 2015

## ABSTRACT

**Purpose** To study the impact of the size and the structure of the nano-assembly on the drug/particle association, determining the intrinsic partition coefficient, in order to better master the encapsulation and release properties of the carrier.

**Methods** An experimental methodology is proposed to characterize the drug/nanoparticle association by mean of a partition coefficient between the PLA-PEG nanoparticles and the suspending aqueous medium, referred to as  $K_p$ . The determination was made from apparent values (referred to as  $K_p^{ap}$ ) measured in the presence of solubilizing agents (albumin and hydroxypropyl- $\beta$ -cyclodextrin) and extrapolation to zero concentration. The structure of nanoparticles was investigated by Transmission Electron Microscopy and static light scattering.

**Results** Depending on the manufacturing process and the PEG length of the copolymer, the nanoparticles structured either as aggregates of copolymer chains or micelles exhibiting significantly different  $K_p$  values.

**Conclusion** The methodological tool described here showed that the difference in cabazitaxel/nanoparticle association between aggregates and micelles could be attributed to the difference in PLA-PEG chains packing.

**KEY WORDS** drug delivery · partition · PLA-PEG nanoparticle · release · static light scattering

## ABBREVIATIONS

a	Length of the lactide monomer repeat unit nm
$a_2$	Excluded volume of the particle nm <sup>3</sup>
$C_{susp}^{BSA}$	Concentration of albumin in the external phase mol/L
$C_{bound}^{drug}$	Concentration of drug bound to the solubilizing agent mg/mL
$C_{diss}^{drug}$	Concentration of drug solubilized in water and associated to the solubilizing agent mg/mL
$C_{free}^{drug}$	Concentration of free drug in the external phase mg/mL
$C_{tot}^{drug}$	Total concentration of drug mg/mL
$C_{susp}^{HP\beta CD}$	Concentration of HP $\beta$ CD in the external phase mol/L
CNaDoc	Concentration of sodium deoxycholate mg/mL
$C_{susp}^{PLA-PEG}$	Concentration of PLA-PEG in the suspension mg/mL
$C_{Acetone}^{PLA-PEG}$	Concentration of PLA-PEG in acetone mg/mL
$C_{CH_2Cl_2}^{PLA-PEG}$	Concentration of PLA-PEG in methylene chloride mg/mL
$C_{susp}^{solub}$	Concentration of solubilizing agent in the suspension mol/L
D	Coefficient of diffusion of nanoparticle nm <sup>2</sup> /s
$d_H$	Hydrodynamic diameter nm
dn/dc	Specific refractive index increment of the PLA-PEG nanoparticles mL/g
$d_{PLA-PEG}$	Bulk density of solid PLA-PEG g/cm <sup>3</sup>
$\eta$	Viscosity of the dispersed medium of nanoparticles Pa.s
g	Correlation function of diffusion
$I_{tol}$	Intensity of light scattered from a toluene solution, used as a reference
$I_{NP}$	Intensity of light scattered from the dispersion

✉ D. Bazile  
Didier.Bazile@sanofi.com

<sup>1</sup> Sanofi Research and Development, Lead Generation to Candidate Realization Platform, 13 Quai Jules Guesde, 94403 Vitry-sur-Seine, France

<sup>2</sup> Laboratoire Léon Brillouin, CEA Saclay, Gif-sur-Yvette Cedex 91191, France

$K'$	Optical constant $\text{mol}\cdot\text{cm}^3/\text{g}^2$
$K_d$	Dissolution constant $\text{mol}/\text{L}$
$K_p$	Partition coefficient between nanoparticle and water
$K_p^{\text{ap}}$	Partition coefficient between nanoparticle and aqueous phase, containing the solubilizing agent
$MA_2$	Second Virial coefficient $\text{cm}^3/\text{g}$
$m_{\text{encaps}}^{\text{drug}}$	Mass of encapsulated cabazitaxel $\text{mg}$
$M_n^{\text{PLA-PEG}}$	Average molecular weight of PLA-PEG $\text{g}/\text{mol}$
$M_w^{\text{NP}}$	Average molecular weight of nanoparticles $\text{g}/\text{mol}$
$N_A$	Avogadro's number $\text{mol}^{-1}$
$N_{\text{agg}}$	Aggregation number of nanoparticle
$N_{\text{PEG}}$	Number of monomer units on PEG
$N_{\text{PLA}}$	Number of monomer units on PLA
$n_{\text{tol}}$	Refractive index of toluene
PDI	Polydispersity index
$q$	Scattering vector $\text{nm}^{-1}$
$R_{\text{core}}$	Core radius of PLA-PEG micelle $\text{nm}$
$R_g$	Radius of gyration of PLA-PEG nanoparticles $\text{nm}$
$R_H$	Hydrodynamic radius of PLA-PEG nanoparticles $\text{nm}$
$R_{\text{tol}}$	Rayleigh ratio of toluene $\text{cm}^{-1}$
$S_{\text{in solub}}^{\text{caba}}$	Maximal solubility of cabazitaxel in solubilizing agent $\mu\text{g}/\text{mL}$
$V_{\text{ext}}$	Volume of the external phase $\text{mL}$
$V_{\text{int}}$	Total volume of nanoparticles $\text{mL}$
$V^{\text{PLA-PEG}}$	Volume occupied by one PLA-PEG chain inside the nanoparticle $\text{nm}^3/\text{molec}$

## INTRODUCTION

While cancer is still a major cause of mortality, nanomedicines appear as a promising approach to decrease the toxicity towards healthy tissues associated to conventional chemotherapeutic treatments (1). As far as the intravenous route is concerned, the design of polymeric nanoparticles exhibiting (i) a prolonged systemic circulation to favor tumor accumulation, by the Enhanced Permeation and Retention (EPR) effect and (ii) a controlled delivery of the drug in the vicinity of the diseased cells, is one of the most reviewed nanotechnology-based anticancer strategies (2,3). Among the nano-objects already tested in clinic, (4) nanoparticles made of PLA-PEG di-block copolymers have some advantages in addition to their long circulating properties (5,6). In preclinical experiments, the PLA was shown to be biodegraded through hydrolysis after intravenous administration within few days, (7) while low molecular weight PEG ( $M_w < 10$  kDa) is thought to be eliminated by renal clearance (8). From an industrial standpoint, the

synthesis of the copolymer by ring-opening polymerization is well-documented and can be performed at multi-gram scale with satisfying purity (9). Finally, the accumulated knowledge of the biopharmacy and the physico-chemistry of these nano-assembled copolymers is another advantage of PLA-PEG nanoparticles. In particular, the density of PEG chains was shown to be critical from a pharmacokinetic (6) and a safety (10) standpoints, while the length of the PLA block was related to the structure of PLA-PEG nanoparticles (11).

The control of the drug/particle association (*i.e.*, the encapsulation during the manufacturing process and the release after *i.v.* administration) is another key aspect of the management of the quality of nano-objects. From an efficacy standpoint, the drug should stay associated to the carrier to be co-delivered in the tumor, and released according to a timescale consistent with the inhibition of cancer cells multiplication (12,13). From a safety standpoint, it is important to note that the biodistribution of the nano-encapsulated drug may be significantly modified as compared to the free drug in solution. Considering that a fraction of the injected dose may accumulate as nanoparticles in undesired organs, (14) the accumulation of the drug in undesired organs is dependent upon the drug/particle association. Moreover, in the systemic circulation, the nano-encapsulated and the free (released) fractions exhibit significantly different biopharmaceutical behaviors. Accordingly, a particular attention is paid to the association of the drug to the nano-carrier, from a regulatory perspective (15,16). Finally, the kinetics of release depends on the dilution of the injected suspension in the blood, the elimination of the free drug, the long circulating properties of the particles and the affinity of the drug for plasma proteins and for the nanoparticles.

Nanoparticles based on a PLA matrix were shown to exhibit satisfactory encapsulating properties for hydrophobic drugs such as taxanes (4,17,18). In previous experiments the association of the drug to the particle was satisfactorily described from the determination of a partition coefficient between the core of the nano-object and the suspending medium (19–21). However, the comparison of published data is often difficult considering (i) the variety of polymers used, (ii) the variety of nano-assembly processes (prone to lead to different nano-objects) and (iii) the suspending conditions that may include surfactants exhibiting solubilizing properties (prone to alter the partition equilibrium). Owing to the low amount of drug available for the early development activities, the nanoprecipitation process, easily miniaturized, is a preferred option at this step, whereas the emulsion-evaporation process may offer more workable options from an industrialization standpoint. While these two processes are alternatively described in the literature to prepare polymeric nanoparticles, data are missing to compare the resulting products in terms of drug/particle association. In practice, the accurate determination of the partition coefficient of hydrophobic drugs exhibiting a satisfactory affinity for the PLA matrix is rendered

difficult due to their poor water solubility. A solubilizing agent, such as serum albumin, can be added to the medium, to increase the apparent solubility of the drug but, in this setting, the partition coefficient is apparent, *i.e.*, dependent upon the experimental conditions (19).

The overall objective of this paper is to investigate the association of cabazitaxel with PLA-PEG nanoparticles, prepared either by nanoprecipitation or emulsion-evaporation with two different PEG-length copolymers.

In a first step, an intrinsic partition coefficient between the nanoparticle and the aqueous suspending buffer was determined combining the partition equilibrium to the binding equilibrium of the drug with a solubilizing agent. Bovine serum albumin and hydroxypropyl  $\beta$ -cyclodextrin (HP $\beta$ CD) were used as solubilizing agent considering their aptness to significantly increase the apparent solubility of cabazitaxel. The “true” (also referred to as “intrinsic”) partition coefficient was derived from the evolution of the experimentally determined “apparent” partition coefficient, as a function of the concentration of solubilizing agent.

In a second step, static light scattering experiments were performed on PLA<sub>30000</sub>-PEG<sub>2000</sub> and PLA<sub>30000</sub>-PEG<sub>5000</sub> nanoparticles prepared by nanoprecipitation or emulsion-evaporation to investigate the influence of the nano-assembly structure on the cabazitaxel/PLA-PEG nanoparticles association. From these experiments, it appears that the partition coefficient may be a satisfactory descriptor of the drug/particle association when appropriate nano-assembly structure is taken into account.

## MATERIALS AND METHODS

### Materials

PLA-PEG<sub>2000</sub> and PLA-PEG<sub>5000</sub> polymers were synthesized at Sanofi (Vitry sur Seine, France). The molecular weights were determined by <sup>1</sup>H NMR, with Bruker spectrometer operating at 600 MHz (NS=128), after solubilization in CDCl<sub>3</sub>:  $M_n^{PLA-PEG2000} = 31\,808$  g/mol and  $M_n^{PLA-PEG5000} = 36\,248$  g/mol. Cabazitaxel was synthesized at Sanofi (Vitry sur Seine, France), ( $M_w = 835$  g/mol). Surfactant: sodium deoxycholate (NaDoc) was from Sigma Aldrich, and hydroxypropyl  $\beta$ -cyclodextrin (HP $\beta$ CD) was from Roquette ( $M_w^{HP\beta CD} = 1500$  g/mol). Bovine Serum Albumin (BSA) was from Sigma Aldrich ( $M_w^{BSA} = 66,000$  g/mol). Solvents: acetone, methylene chloride and acetonitrile were from Carlo Erba Reactifs (France).

### Nanoparticles Preparation

The PLA-PEG nanoparticles were prepared either by nanoprecipitation or emulsion-evaporation. In both cases,

the copolymer was dissolved into the organic phase at a 2–10 mg/mL (nanoprecipitation) or a 30 mg/mL (emulsion-evaporation) concentration along with cabazitaxel at a concentration corresponding to 5% *w/w* of the polymer concentration. Surfactant (NaDoc) was introduced in the aqueous phase at a 0.2 or 1 mg/mL concentration.

For nanoprecipitation, 25 mL of PLA-PEG/Cabazitaxel acetone solution was added to 75 mL of aqueous phase at a 5 mL/min controlled rate using a HPLC pump, under blade stirring (300 rpm).

For emulsion-evaporation, 100 mL of PLA-PEG/Cabazitaxel methylene chloride solution was emulsified in 300 mL of aqueous phase, using an Ika® Ultra-turrax® (working at 1500 rpm) over ice for 5 min and 15 cycles of High Pressure Homogenizer (M-110S Laboratory Microfluidizer®, Microfluidics).

For both processes, the solvent was then evaporated using a rotary evaporator (pressure was carefully scaled down to 20 mbar and water bath was heated at 35°C). The complete removal of solvent was verified by gas chromatography. Purification and concentration steps were done immediately after preparation by tangential flow filtration (polyethersulfone membrane,  $M_{wc} = 100$  kD, Pall) and by ultracentrifugation (Optima Max, Beckmann Coulter) for 1 h at 59,573 G for emulsion-evaporation and by filtration-centrifugation (Hydrosart®, stabilized cellulose membrane,  $M_{wc} = 10$  kD, Amicon Vivascience) for nanoprecipitation. After purification, nanoparticles were suspended in water.

### Nanoparticles Composition

*Cabazitaxel loading:* the concentration of cabazitaxel was determined by HPLC using a Luna C18 Phenomenex, 3  $\mu$ m column, thermostated at 40°C, after dissolution of nanoparticles in ACN (10 to 50 times dilution of suspensions). The elution flow rate was 1 mL/min and the injected volume was 20  $\mu$ L. The mobile phase was a 65/35 mixture of ACN/water+0.1% *w/w* TFA, used in an isocratic mode. Elution was monitored by UV detection at 230 nm. The retention time for cabazitaxel was 5.2 min. The reference samples of cabazitaxel in ACN were prepared to plot the calibration curve and the linearity was assessed over a concentration range 5–100  $\mu$ g/mL ( $y = 22436x$ ,  $r^2 = 0.9998$ ). The accuracy of cabazitaxel concentration determination was evaluated to be CV=2% (repeatability of reference sample at 31  $\mu$ g/mL).

*Polymer:* the concentration of polymer was determined by Size Exclusion Chromatography (SEC) using a Phenomenex Phenogel 5  $\mu$ m 10<sup>3</sup>A column, thermostated at 35°C. Aqueous suspensions obtained from concentration or lyophilisates were dissolved in ACN. The elution flow rate was 1 mL/min and the injection volume was 20  $\mu$ L. The injections were performed in duplicate.

Elution in ACN was monitored by UV (230 nm) and RI detections. The accuracy of polymer concentration determination was evaluated to be CV=5% when  $C^{PLA-PEG} > 2$  mg/mL. The signal to noise ratio was increased using PLA-PEG samples concentrated after drying by freeze-drying.

### Physico-Chemical Characterization

The hydrodynamic diameter ( $d_H$ ) and polydispersity index (PDI) of nanoparticles were measured by quasi elastic light scattering, using a Zetasizer Nano ZS instrument (Malvern, France). Suspensions were diluted in water for injection. Measurements were performed in duplicate at 20°C, at a 173° angle to avoid multiple scattering. The counting time was set automatically. The analysis was performed using the Cumulant method.

Transmission Electron Microscopy was performed using a Jeol operating at 80 kV. Uranyl acetate was added to the nanoparticles as negative stain and the suspension (5–10 mg/mL) was deposited on grid.

Static Light Scattering measurements were performed in Laboratoire Léon Brillouin (LLB, Saclay, France) using a homemade spectrometer, which consisted in a linear polarized laser with a wavelength of  $\lambda_0 = 515$  nm and a correlator Correlator.com. Suspensions were filtered through 0.45  $\mu$ m and placed in a cylindrical glass cell (2 × 10 cm) kept at room temperature. Three successive dilutions were performed in the same cell by introducing 0.22  $\mu$ m filtered water. The scattering intensity was measured for 1 min at 20 angles to the incident beam in the 20°–150° range.

According to the Rayleigh-Gans-Debye equation:

$$\frac{I_{NP}(q)R_{tol}}{I_{tol}(q)K' C_{susp}^{PLA-PEG}} = M_w^{NP} \left( 1 - \frac{q^2 R_g^2}{3} + \dots \right) \left( 1 - 2MA_2 C_{susp}^{PLA-PEG} + \dots \right) \tag{1}$$

where

- $I_{tol}$  is the intensity of light scattered from a toluene solution, used as a reference ( $I_{tol} = 1032$ )
- $I_{NP}$  is the intensity of light scattered from the dispersion (corrected for the scattering from the solvent)
- $M_w^{NP}$  is the average molecular weight of nanoparticles (g/mol)
- $MA_2$  is the second Virial coefficient
- $C_{susp}^{PLA-PEG}$  is the concentration of PLA-PEG nanoparticles in the suspension (mg/mL)
- $R_g$  is the radius of gyration of PLA-PEG nanoparticles (nm)
- $q$  is the scattering vector.

The optical constant  $K'$  or contrast was given by:

$$K' = \frac{4\pi^2 n_{tol}^2}{N_A \lambda_0^4 R_{tol}} \left( \frac{dn}{dc} \right)^2 \tag{2}$$

where

- $n_{tol}$  and  $R_{tol}$  are the refractive index and Rayleigh ratio of toluene
- $N_A$  is the Avogadro's number
- $dn/dc$  is the specific refractive index increment of the PLA-PEG nanoparticles,  $dn/dc = 0.108$  mL/g (11).

Using Guinier approximation, in diluted regime ( $qR_g \ll 1$ ), for a given concentration of nanoparticles:

$$I_{NP}(q) = I_0 \exp \left( - \frac{q^2 R_g^2}{3} \right) \tag{3}$$

The smaller measurable  $R_g$  was expressed as:

$$R_{g \min} = \sqrt{\frac{dI}{I}} \times \sqrt{\frac{3}{q_{max}^2}} \tag{4}$$

With 5% experimental error on intensity at  $q_{max} = 0.03$  nm<sup>-1</sup>, this resulted in  $R_{g \min} = 13$  nm.

Extrapolation to zero angle of observation of Eq. 1 resulted in:

$$M_{app} \left( C_{susp}^{PLA-PEG} \right) = \frac{I_0 R_{tol}}{I_{tol} K' C_{susp}^{PLA-PEG}} = M_w^{NP} \left( 1 - 2MA_2 C_{susp}^{PLA-PEG} \right) \tag{5}$$

$$\lim_{C_{susp}^{PLA-PEG} \rightarrow 0} \frac{I_0 R_{tol}}{I_{tol} K' C_{susp}^{PLA-PEG}} = M_w^{NP}$$

Dynamic light scattering experiments were performed in the same set of experiments. The correlation functions (g) obtained at different angles *versus*  $tq^2$  overlaid, confirming the diffusive motion of nanoparticles in suspension. The coefficient of diffusion, D, was deduced from the equation:

$$g = \beta \cdot \exp(-2Dtq^2) + 1 \tag{6}$$

Then, the hydrodynamic radius of nanoparticles,  $R_H$ , was given by:

$$R_H = \frac{k_B T}{6\pi\eta D} \tag{7}$$

Where  $\eta$  is the viscosity of the dispersed medium of nanoparticles.

## Partition Coefficient Determination

Unbound NaDoc was removed from PLA-PEG nanoparticles suspensions by ultracentrifugation and the nanoparticles were re-suspended in water for injection. When the nanoparticles were too small to be separated by ultracentrifugation and re-suspended in water, the concentration of NaDoc was decreased by filtration-centrifugation at a level below the critical micellar concentration of NaDoc (*i.e.*,  $C^{\text{NaDoc}} = 1 \text{ mg/mL}$ ) (22) so that drug solubilization by Nadoc was not likely.

The nanoparticles were diluted in the range of concentration  $C_{\text{susp}}^{\text{PLA-PEG}} = 0.5\text{--}10 \text{ mg/mL}$  in solutions of hydroxypropyl  $\beta$ -cyclodextrin ( $C_{\text{susp}}^{\text{HP}\beta\text{CD}} = 3.3, 6.67 \text{ and } 13.3 \text{ mM}$ ) or albumin ( $C_{\text{susp}}^{\text{BSA}} = 0.303, 0.606, 0.909 \text{ and/or } 1.21 \text{ mM}$ ) in Tris-buffer. The samples were incubated under mild stirring at  $37^\circ\text{C}$  for 2.5 h. The drug was present in different forms: (i) the drug encapsulated in the nanoparticle, (ii) the drug solubilized in water, (iii) the drug associated to the solubilizing agent and (iv) the precipitated drug (Fig. 1).

At the equilibrium, the partition coefficient,  $K_p$  and dissolution constant,  $K_d$  were defined as:

$$K_p = \frac{m_{\text{encaps}}^{\text{drug}}}{C_{\text{free}}^{\text{drug}} V_{\text{int}}} \text{ and } K_d = \frac{C_{\text{free}}^{\text{drug}} C_{\text{susp}}^{\text{solub}}}{C_{\text{bound}}^{\text{drug}}} \quad (8)$$

where

- $m_{\text{encaps}}^{\text{drug}}$  is the mass of encapsulated cabazitaxel (mg)
- $C_{\text{free}}^{\text{drug}}$  is the concentration of free cabazitaxel in the external phase (mg/mL)
- $C_{\text{bound}}^{\text{drug}}$  is the concentration of cabazitaxel, bound to the solubilizing agent in the external phase (mg/mL)
- $C_{\text{susp}}^{\text{solub}}$  is the concentration of solubilizing agent in the suspension (mol/L)
- $V_{\text{int}}$  is the internal volume of nanoparticles (mL).

The dissociation constants of cabazitaxel in albumin,  $K_d^{\text{BSA}}$  and HP $\beta$ CD solutions,  $K_d^{\text{HP}\beta\text{CD}}$ , were determined

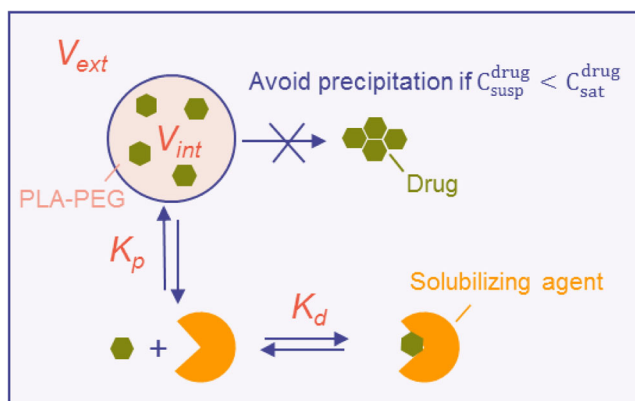


**Fig. 1** Schematic representation of the cabazitaxel forms.

experimentally from the maximal solubility of cabazitaxel ( $S_{\text{in solub}}^{\text{caba}}$ ) in BSA and HP $\beta$ CD solutions of varying concentrations  $C_{\text{susp}}^{\text{solub}}$  and the Eq. 9:

$$S_{\text{in solub}}^{\text{caba}} = S_{\text{in water}}^{\text{caba}} \left( 1 + \frac{C_{\text{susp}}^{\text{solub}}}{K_d} \right) \quad (9)$$

$$S_{\text{in water}}^{\text{caba}} = 8 \text{ } \mu\text{g/mL}$$

The determination led to:

$$K_d^{\text{BSA}} = 6.8 \cdot 10^{-4} \text{ mol/L}$$

$$K_d^{\text{HP}\beta\text{CD}} = 10.35 \cdot 10^{-4} \text{ mol/L}$$

The accuracy for  $K_d$  was determined analytically to be  $\Delta K_d/K_d = 8\%$ .

The amounts of the cabazitaxel forms (encapsulated, bound to the solubilizing agent and free) can be summed up according to the law of mass conservation:

$$(V_{\text{int}} + V_{\text{ext}}) C_{\text{tot}}^{\text{drug}} = K_p C_{\text{free}}^{\text{drug}} V_{\text{int}} + C_{\text{free}}^{\text{drug}} V_{\text{ext}} + V_{\text{ext}} C_{\text{free}}^{\text{drug}} C_{\text{susp}}^{\text{solub}} / K_d \quad (10)$$

Where  $C_{\text{tot}}^{\text{drug}}$  is the total concentration of cabazitaxel (mg/mL).

Introducing the apparent partition coefficient,  $K_p^{\text{ap}}$ , as the partition coefficient between the nanoparticle and the aqueous phase, containing the solubilizing agent and  $C_{\text{diss}}^{\text{drug}} = C_{\text{bound}}^{\text{drug}} + C_{\text{free}}^{\text{drug}}$

$$K_p^{\text{ap}} = \frac{m_{\text{encaps}}^{\text{drug}}}{C_{\text{diss}}^{\text{drug}} V_{\text{int}}} \quad (11)$$

$$K_p^{\text{ap}} = \frac{K_p K_d}{K_d + C_{\text{susp}}^{\text{solub}}} \quad (12)$$

Assuming the suspension was diluted,  $V_{\text{int}} \ll V_{\text{ext}}$ , the law of mass conservation can be written as:

$$\frac{C_{\text{tot}}^{\text{drug}}}{C_{\text{diss}}^{\text{drug}}} = 1 + K_p^{\text{ap}} \frac{C_{\text{susp}}^{\text{PLA-PEG}}}{d_{\text{PLA-PEG}}} \quad (13)$$

where

$C_{\text{susp}}^{\text{PLA-PEG}}$  is the concentration of polymer in the suspension (mg/mL), measured by SEC after dissolution of nanoparticles in ACN as described above

$d_{\text{PLA-PEG}}$  is the bulk density of solid PLA-PEG. It was assumed to be the same for all types of nanoparticles and equal to the reported value of PLA amorphous solid:  $1.25 \text{ g/cm}^3$  (23).

After reaching the thermodynamic equilibrium, the fraction of cabazitaxel released from the PLA-PEG nanoparticles (*i.e.*, free and bound to the solubilizing agent, referred to as  $C_{diss}^{drug}$ ), was separated from the encapsulated cabazitaxel fraction by ultracentrifugation (50 000 rpm to 90 000 rpm 30 min) and quantified by HPLC using the method described above, whereas PLA-PEG concentration was determined by SEC.

The apparent partition coefficient,  $K_p^{ap}$  for various concentrations of HP $\beta$ CD and BSA, were determined from the plot of  $C_{tot}^{drug}/C_{diss}^{drug}$  versus  $C_{susp}^{PLA-PEG}/d_{PLA-PEG}$ , according to Eq. 13, while the plot of  $K_p^{ap}$  versus  $K_d/(K_d + C_{susp}^{solub})$  leads to  $K_p$ , according to Eq. 12.

## RESULTS

### Nanoparticles Preparation and Characterization

The size, PDI and composition of PLA-PEG/cabazitaxel nanoparticles prepared either with PLA-PEG<sub>2000</sub> or PLA-PEG<sub>5000</sub>, by nanoprecipitation, using different PLA-PEG concentrations in acetone ( $C_{Acetone}^{PLA-PEG}$ ), or emulsion-evaporation, were reported in the Tables I and II.

For all manufacturing conditions, slight aggregation of nanoparticles was noticed. For nanoprecipitation, the size of nanoparticles varied from 27 to 54 nm and was mostly dependent on the type of polymer. The nanoparticles were homogeneous in size as denoted by low PDI (PDI < 0.20). The nanoparticles prepared by emulsion-evaporation were bigger, as compared to nanoprecipitation, from 126 to 155 nm, and the PDI was low (Table II).

For nanoprecipitation and emulsion-evaporation, the experimental drug loadings were determined (Tables I and II) and compared to the targeted 5% *w/w* loading, adjusted from the initial ratio of  $C_{tot}^{drug}/C_{susp}^{PLA-PEG}$  (see “Materials and Methods”). For nanoprecipitation, the experimental drug loading varied from 4.9% *w/w* to 6.0% *w/w*, as a function of the copolymer and the manufacturing conditions. The higher values of experimental drug loading, as compared to targeted value (5% *w/w*), can be explained by the loss of

**Table I** Characterization of PLA-PEG<sub>2000</sub> and PLA-PEG<sub>5000</sub> Nanoparticles, Produced by Nanoprecipitation, Using Different Formulation Conditions

Nanoprecipitation	$C_{Acetone}^{PLA-PEG}$ (mg/mL)	$C^{NaDoc}$ (mg/mL)	$d_H$ (nm)	PDI	Loading <sup>exp a</sup> (% <i>w/w</i> )
PLA-PEG <sub>2000</sub>	2	0.2	37	0.03	4.9
	10		54	0.11	5.2
PLA-PEG <sub>5000</sub>	2	0.2	31	0.09	5.1
	10		27	0.10	6.0

<sup>a</sup> Experimental drug loading was calculated as  $C_{tot}^{drug}/C_{susp}^{PLA-PEG}$  and can be compared to the targeted drug loading of 5% *w/w*

**Table II** Characterization of PLA-PEG<sub>2000</sub> and PLA-PEG<sub>5000</sub> Nanoparticles, Produced by Emulsion-Evaporation Process in Duplicate

Emulsion-evaporation	$C_{CH2Cl2}^{PLA-PEG}$ (mg/mL)	$C^{NaDoc}$ (mg/mL)	$d_H$ (nm)	PDI	Loading <sup>exp a</sup> (% <i>w/w</i> )
PLA-PEG <sub>2000</sub>	30	1	126	0.10	4.9
			155	0.17	4.8
PLA-PEG <sub>5000</sub>	30	1	141	0.02	5.0
			142	0.09	4.6

<sup>a</sup> Experimental drug loading was calculated as  $C_{tot}^{drug}/C_{susp}^{PLA-PEG}$  and can be compared to the targeted drug loading of 5% *w/w*

polymer during the nano-assembling process, as suggested by the aggregation observed after solvent evaporation. For emulsion-evaporation, the experimental drug loading was comprised between 4.6% *w/w* and 5.0% *w/w* and was not significantly dependent on the type of PLA-PEG.

### Determination of Partition Coefficient

The PLA-PEG nanoparticles, produced by nanoprecipitation (with  $C_{Acetone}^{PLA-PEG} = 10$  mg/mL) or emulsion-evaporation process, were dispersed in BSA or HP $\beta$ CD solutions, as described in the materials and methods. The plot of  $C_{tot}^{drug}/C_{diss}^{drug}$  versus  $C_{susp}^{PLA-PEG}/d_{PLA-PEG}$  obtained for each partition condition gives a straight line ( $r^2$  ranged from 0.84 to 0.999) from which  $K_p^{ap}$  was determined by linear regression (Eq. 13). Only PLA-PEG<sub>2000</sub> nanoparticles prepared by nanoprecipitation were exemplified on Fig. 2. The same trend was observed for the other samples.

For PLA-PEG<sub>2000</sub> nanoparticles produced by nanoprecipitation and emulsion-evaporation, the slope of the linear regression of the plot of  $K_p^{ap}$  as a function of  $K_d/(K_d + C_{susp}^{solub})$ , obtained with varying concentrations of HP $\beta$ CD and BSA, was not dependent on the solubilizing agent (Eq. 12, Fig. 3). The fit was considered satisfactory since for the 2 types of nanoparticles, the regression coefficients  $r^2$  were higher or equal to 0.98. Therefore, the partition coefficient  $K_p$  between nanoparticles, produced by nanoprecipitation and emulsion-evaporation with PLA-PEG<sub>2000</sub> and PLA-PEG<sub>5000</sub>, and water was determined from the slope of the linear regression of the plot of  $K_p^{ap}$  as a function of  $K_d/(K_d + C_{susp}^{solub})$ , obtained with varying concentrations of HP $\beta$ CD (Fig. 4, Table III). The fit was considered satisfactory since for the 4 types of nanoparticles, the regression coefficients  $r^2$  were higher than 0.996. Moreover, the hypothesis of partition equilibrium, which considers complete release of cabazitaxel at infinite concentration of solubilizing agent, was consistent with the null  $y$ -intercept.

For the emulsion-evaporation process,  $K_p$  was equal to 9578 and 8643, for PLA-PEG<sub>2000</sub> and PLA-PEG<sub>5000</sub>, respectively. Considering the analytically determined accuracy on  $K_p$  ( $\Delta K_p/K_p = 11\%$ ),  $K_p$  did not significantly depend on the type of polymer used, *e.g.*, on the length of the PEG chain. The

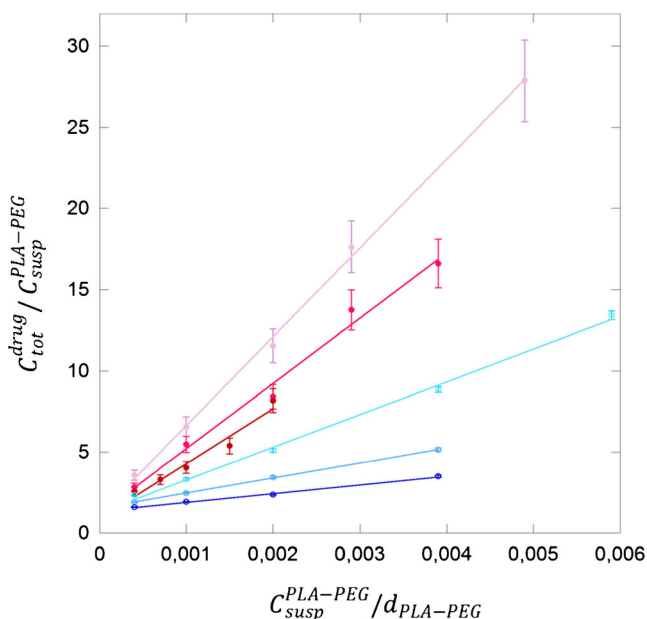


**Fig. 2** Experimental points (filled circles) and linear regressions (plain curves) for the ratio  $C_{tot}^{drug}/C_{diss}^{drug}$  versus  $C_{susp}^{PLA-PEG}/d_{PLA-PEG}$  obtained for separate dilutions of PLA-PEG<sub>2000</sub> nanoparticles produced by nanoprecipitation in solutions of HPβCD (in blue,  $C_{susp}^{HP\beta CD} = 3.3, 6.67$  and  $13.3$  mM) or albumin (in red,  $C_{susp}^{BSA} = 0.303, 0.606$  and  $0.909$  mM).

$K_p$  was slightly decreased when nanoparticles were formed with PLA-PEG<sub>2000</sub> by nanoprecipitation. But more interestingly,  $K_p$  was 1.5 times higher when nanoprecipitation was chosen versus emulsion-evaporation for PLA-PEG<sub>5000</sub>, which denotes a higher affinity of the drug for the nanoparticle. At the same time, PLA-PEG<sub>5000</sub> nanoparticles prepared by

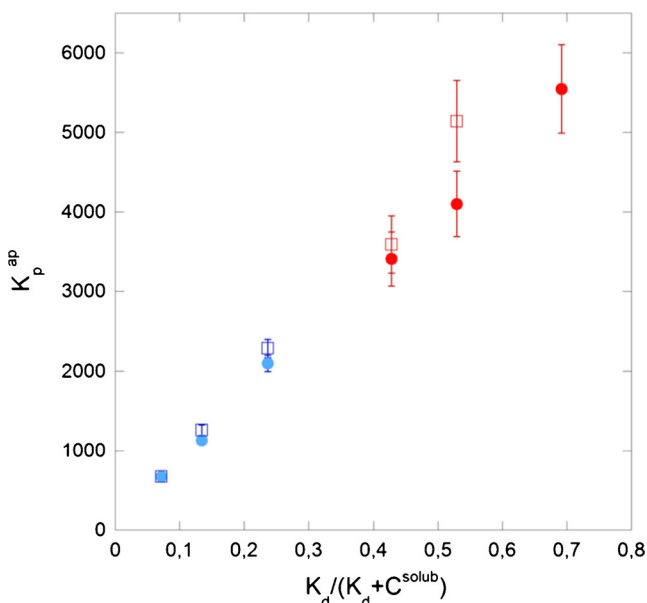


**Fig. 3** Apparent partition coefficient,  $K_p^{ap}$ , versus  $K_d/(K_d + C_{susp}^{solub})$  obtained for PLA-PEG<sub>2000</sub> nanoparticles produced by nanoprecipitation (filled circles) and emulsion-evaporation (open squares) in solutions of HPβCD (blue) and BSA (red).

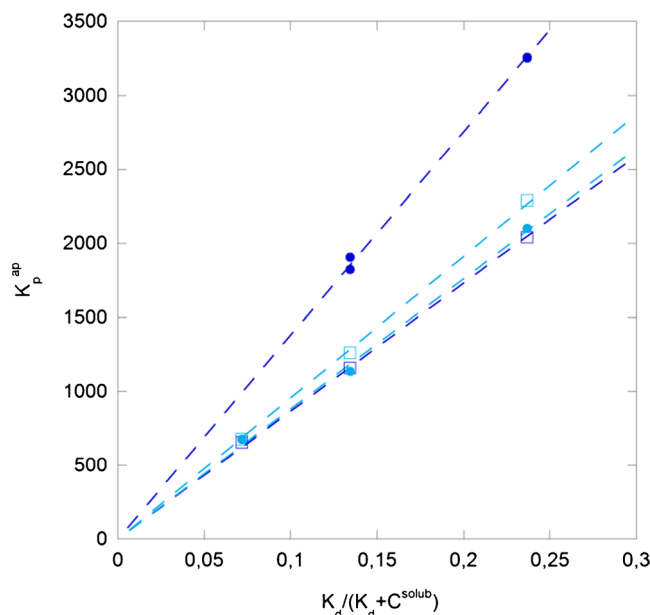


**Fig. 4** Apparent partition coefficient,  $K_p^{ap}$ , versus  $K_d/(K_d + C_{susp}^{solub})$  obtained for PLA-PEG<sub>2000</sub> (light blue) and PLA-PEG<sub>5000</sub> (dark blue) nanoparticles produced by nanoprecipitation (filled circles) and emulsion-evaporation (open squares) in solutions of HPβCD.

nanoprecipitation were significantly smaller (approximately 5 times), which suggests that the favored interaction between cabazitaxel and PLA-PEG was related to the structure of the nano-object, more precisely to a different arrangement of PLA-PEG chains inside the smallest nanoparticles.

### Structure of Nanoparticles

Therefore, the relationship between the structure of the nanoparticles and the partition coefficient was investigated. The PLA-PEG/cabazitaxel nanoparticles morphology was studied in a first step by Transmission Electron Microscopy (TEM). The spherical shape of nanoparticles was evidenced for nanoparticles prepared by both processes and the sizes evaluated by microscopy were in good agreement with the hydrodynamic diameter,  $d_H$ , measured by dynamic light scattering (Fig. 5). Static Light Scattering (SLS) experiments were performed in a

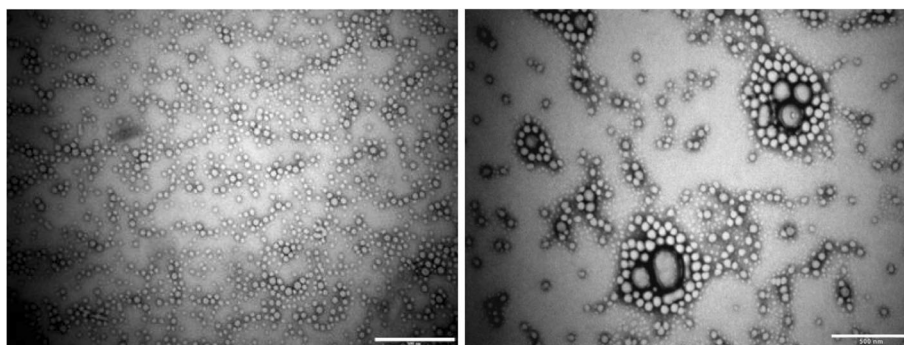
**Table III** Partition Coefficients,  $K_p$ , for PLA-PEG Nanoparticles of Hydrodynamic Diameters,  $d_H$ .  $r^2$  was the Regression Coefficient of Linear Equation

Polymer	PLA-PEG <sub>2000</sub>	PLA-PEG <sub>5000</sub>	PLA-PEG <sub>2000</sub>	PLA-PEG <sub>5000</sub>
Process	Emulsion-evaporation	Emulsion-evaporation	Nanoprecipitation <sup>a</sup>	Nanoprecipitation <sup>a</sup>
$d_H$ (nm)	126	141	54	27
$K_p$	9578	8643	8805	13 772
$r^2$	0.999	0.999	0.996	0.998

<sup>a</sup> For nanoprecipitation,  $C_{Acetone}^{PLA-PEG} = 10$  mg/mL

<sup>b</sup> Theoretical max loading was calculated from Eq. 19

**Fig. 5** TEM pictures of PLA-PEG<sub>2000</sub>/cabazitaxel nanoparticles produced by nanoprecipitation (*left*) and emulsion-evaporation (*right*), for magnification 50 K (scale bar 500 nm).



second step to investigate the composition of nanoparticles, in terms of number of PLA-PEG chains packed together.

The angular dependence of the light scattering intensity for nanoparticles, produced by nanoprecipitation and emulsion-evaporation, with PLA-PEG<sub>2000</sub> and PLA-PEG<sub>5000</sub> was shown in the Fig. 6, left and right panels respectively. As

expected, the smaller PLA-PEG<sub>5000</sub> nanoparticles ( $R_H = 13 \text{ nm}$ ;  $< \lambda/20$ ) behaved like point scatterers and the corresponding scattering profiles were almost anisotropic (Fig. 6, top right). On the opposite, q-dependent scattered intensity was evidenced for the 3 other types of nanoparticles, as expected for interparticles interactions.

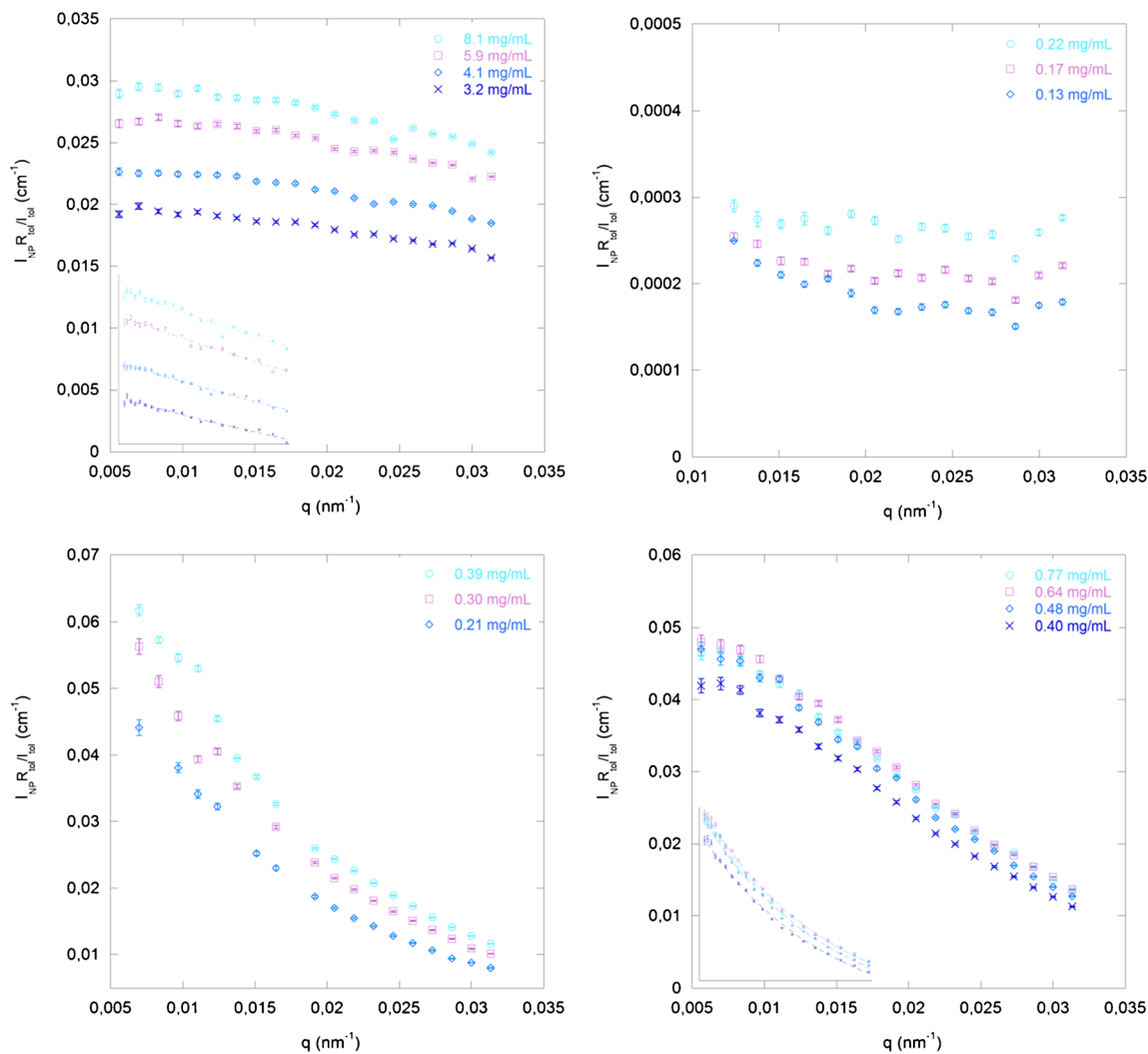


**Fig. 6** Scattered intensity curves for nanoparticles produced by nanoprecipitation (*top*) and emulsion-evaporation (*down*), respectively with PLA-PEG<sub>2000</sub> (*left*) and PLA-PEG<sub>5000</sub> (*right*). Insets:  $I$  versus  $q^2$  fitted by exponential decrease. Legend:  $\text{PLA-PEG}_{\text{susp}}$



The scattering profiles were fitted using Guinier approximation (Eq. 1) and the radius of gyration,  $R_g$ , was determined. Extrapolations of the scattering intensity, to zero angle of observation and infinite dilution, yielded the second virial coefficient  $MA_2$  and the average molecular weight of nanoparticles  $M_w^{NP}$  (Eq. 5, Table IV). The second virial coefficient,  $MA_2$ , is an inter-particle interaction parameter. A positive value, for the 4 samples, denoted repulsion between nanoparticles. Accordingly, satisfactory colloidal stability was observed, even in stress conditions (data not shown). Values of  $M_w^{NP}$  were used to calculate the aggregation number of particles, as  $N_{agg} = M_w^{NP}/M_n^{PLA-PEG}$  (using  $M_n^{PLA-PEG}$  obtained by NMR, see “Materials” section). For emulsion-evaporation, the aggregation number was of the same order of magnitude for PLA-PEG<sub>2000</sub> and PLA-PEG<sub>5000</sub>. For nanoprecipitation, the aggregation number was 25 times lower as compared to emulsion-evaporation, for PLA-PEG<sub>2000</sub> and 112 times lower for PLA-PEG<sub>5000</sub>. Finally, the excluded volume of the particle, defined as  $a_2 = M_w^{NP}MA_2/N_a$  and describing the intensity of repulsive interactions, was 100 times higher for nanoparticles produced by emulsion-evaporation as compared to nanoprecipitation, due to the respective size of the objects. However, for a given process,  $a_2$  was higher for PLA-PEG<sub>5000</sub> than for PLA-PEG<sub>2000</sub> nanoparticles. As expected, the longer the PEG chains, the higher the steric repulsion between particles.

## DISCUSSION

### Influence of the Process on the Structure of Nanoparticles

The nanoprecipitation is a spontaneous process, which does not require energy input. It is based on the Ouzo effect, (24,25) which occurs upon mixing of a water-miscible solvent, containing a low amount of a hydrophobic specie (e.g., polymer), to a large volume of water. Nanoparticles formation resulted in different mechanisms: nucleation, growth and Ostwald ripening. The resulting nanoparticle size and polydispersity, drug loading and encapsulation efficiency were shown to be dependent on experimental conditions, such as

the nature and volume fraction of water-miscible solvent, the concentration of polymer and the relative solubility of drug in water as compared to the solvent (26,27). In the experiments described here, acetone was chosen as an appropriate water-miscible solvent since it is consistent with  $\theta$  conditions for PLA, (28) and the solubility of cabazitaxel was 10 000 times higher in acetone than in water. The concentration of polymer,  $C_{Acetone}^{PLA-PEG}$  varied from 2 to 10 mg/mL. For PLA-PEG<sub>5000</sub>, the nanoparticles were very small and their size did not depend on  $C_{Acetone}^{PLA-PEG}$  (Table I). We concluded that the nano-objects were micelles made of a PLA core and a PEG shell, as already described by Riley *et al.* (11) (Fig. 7a). This hypothesis was in good agreement with the low aggregation number of PLA-PEG<sub>5000</sub> nanoparticles formed at  $C_{Acetone}^{PLA-PEG} = 10$  mg/mL (Table IV). More specifically, considering the length of the hydrophobic PLA block,  $N_{PLA} = 417$  units, as compared to the length of the hydrophilic PEG block,  $N_{PEG} = 114$  units, the PLA-PEG<sub>5000</sub> nanoparticles are most likely crew-cut micelles, and the following relations may apply: (29)

$$N_{agg} \sim N_{PLA} \quad (14)$$

$$R_{core} \sim aN_{PLA}^{2/3} \quad (15)$$

Where  $a$  is the length of the lactide monomer repeat unit

The theoretical core radius,  $R_{core}$ , of PLA-PEG<sub>5000</sub> micelle was 10.6 nm. The surface area occupied by one PEG<sub>5000</sub> chain was calculated by dividing the mean surface area of the nanoparticles ( $4\pi R_{core}^2$ ) by the aggregation number,  $N_{agg}$ , which led to 7.0 nm<sup>2</sup>. The corresponding distance between two PEG<sub>5000</sub> chains was  $d_{PEG} = 2.6$  nm. The PEG chains conformation can be deduced by comparing the distance  $d_{PEG}$  to the Flory radius of PEG in good solvent ( $R_F = 6.1$  nm), as already done by Louguet *et al.* (30). The distance  $d_{PEG}$  being smaller than  $R_F$ , suggests that the PEG chains strongly interact with each other and were forced to stretch away from the surface of micelle adopting a brush conformation. The hydrophilic shell formed with PEG<sub>5000</sub> in brush, is related to the good colloidal stability of micelles, already illustrated by the high value of  $a_2$  (Table IV) (31,32).

**Table IV** Size, Average Molecular Weight and Second Virial Coefficient of PLA-PEG Nanoparticles as Determined by Static Light Scattering

Process	Polymer	$R_H$ (nm)	$R_g$ (nm)	$M_w^{NP} \times 10^{-7}$ (g/mol)	$N_{agg}$	$MA_2$ (cm <sup>3</sup> /g)	$a_2 \times 10^{-6}$ (nm <sup>3</sup> )
EE	PLA-PEG <sub>2000</sub>	80	69	100	31 439	402	668
EE	PLA-PEG <sub>5000</sub>	73	63	81.7	22 539	578	784
NPr	PLA-PEG <sub>2000</sub>	28	26	4.01	1 261	33	2.2
NPr	PLA-PEG <sub>5000</sub>	13	–	0.73	201	389	4.7

EE emulsion-evaporation and NPr nanoprecipitation with  $C_{Acetone}^{PLA-PEG} = 10$  mg/mL

$R_H$ : DLS measurement of filtrated and diluted sample at 90° and using Eq. 7

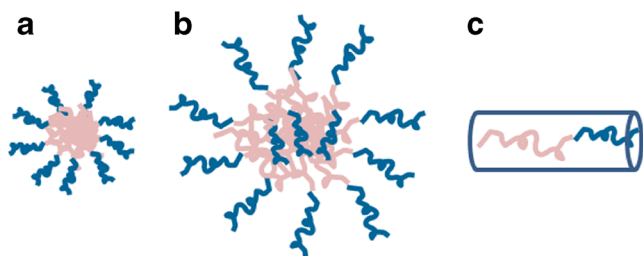


**Fig. 7** Schematic representations of (a) PLA-PEG micelle; (b) Nano-assembly of aggregated PLA and PEG chains and (c) Volume occupied by one PLA-PEG chain.

For PLA-PEG<sub>2000</sub>, the nanoparticles were bigger and the size depended on the concentration of polymer in acetone (Table I). According to the previous considerations, these nanoparticles cannot be structured as micelles. Indeed, when nanoparticles were prepared with  $C_{Acetone}^{PLA-PEG} = 10$  mg/mL, the aggregation number ( $N_{agg}$ ) was 6 times higher as compared to the value obtained for PLA-PEG<sub>5000</sub> micelle and the assemblies were 2 times bigger ( $R_H$ ), while the length of the hydrophobic PLA block ( $N_{PLA}$ ) was constant. The nanoparticles were more likely aggregates of copolymer chains (Fig. 7b), a fraction of PEG chains being embedded in the core of the nanoparticles, as evidenced by Karnik *et al.* (33).

The emulsion-evaporation process requires the use of specific equipment, such as high pressure homogenizer, with high energy consumption and usually higher amount of surfactant, as compared to nanoprecipitation, to avoid emulsion destabilization, by coalescence for instance. The size and polydispersity of nanoparticles mainly depended on the shear force applied to the emulsion and the concentration of surfactant. (34) In the experiments described here, the optimization of the experimental conditions led to the formation of 140 nm mean diameter nanoparticles for both PLA-PEG<sub>2000</sub> and PLA-PEG<sub>5000</sub>. Methylene chloride was considered as an appropriate solvent as the solubility of cabazitaxel was 5000 times higher, as compared to water. The partition of the drug was therefore strongly in favor of the organic phase. The aggregation numbers of resulted nanoparticles were 113 times higher for PLA-PEG<sub>5000</sub> and 25 times higher for PLA-PEG<sub>2000</sub> as compared to nanoparticles produced by nanoprecipitation (Table IV). We concluded that, both polymers produced, by emulsion-evaporation, nano-assembled as aggregates of PLA and PEG chains (Fig. 7b).

### Influence of the Structure on the Partition Coefficient

The volume occupied by one PLA-PEG chain inside the nanoparticle:  $V^{PLA-PEG}$  (Fig. 7c) can be calculated for nanoparticles made of aggregates and micelle from:

$$V^{PLA-PEG} = \frac{4\pi R_H^3}{3N_{agg}} \quad (16)$$

For the three studied nanoparticles made of aggregates  $V_{PLA-PEG}$  was similar, the corresponding values were close to  $70 \text{ nm}^3/\text{molecule}$  (Table V). Consistently,  $R_H/R_g$  was comprised between 1.1 and 1.2, which was close to the theoretical value of coil ( $R_H/R_g = 1.2$ ). The network of PLA chains inside nanoparticles was probably swelled with PEG chains.

For micelles,  $V^{PLA-PEG}$  was 1.6 times smaller as compared to the nanoparticles made of aggregates (Table V). We concluded that the copolymer chains were more packed in the micelles. Unfortunately, the theoretical value of  $R_H/R_g = 1.3$  of dense hard sphere could not be verified with micelle in these experiments, since  $R_g$  cannot be measured. In fact, the hydrodynamic radius of micelles ( $R_H = 13 \text{ nm}$ ) was close to the minimal measurable  $R_g$  by SLS (see “Materials and Methods”). The Small Angle Neutron Scattering would be more appropriate technique for this type of nanoparticle (35,36). The structure of nanoparticles was then related to the affinity of cabazitaxel for the PLA-PEG nano-object. In this attempt, the new experimental methodology presented, was set up to determine the partition coefficient,  $K_p$ , of cabazitaxel between PLA-PEG nanoparticle and water, by the intermediate measurement of an apparent partition coefficient in presence of solubilizing agent. The methodology was validated by linearity of encapsulated *versus* free fraction of drug with two solubilizing agents (HP $\beta$ CD and BSA). It is worth mentioning that, this methodology could be used in any biorelevant media, such as plasma. Considering the parameters reported in the Table V together with the above conclusions on nanoparticle structure, micelle nanoparticles were characterized by a partition coefficient,  $K_p$ , 1.6 times higher than aggregate nanoparticles, suggesting that the interactions between cabazitaxel and nanoparticle were favored. Interestingly, a correlation

**Table V** Structure and Affinity Parameters for Different PLA-PEG Nanoparticles

Process	Polymer	$R_H$ (nm)	$R_H/R_g$	$N_{agg}$	Structure	$V^{PLA-PEG}$ ( $\text{nm}^3/\text{molecule}$ )	$K_p$
EE	PLA-PEG <sub>2000</sub>	80	1.2	31 439	Aggregate NP	68	9578
EE	PLA-PEG <sub>5000</sub>	73	1.2	22 539	Aggregate NP	72	8643
NPr	PLA-PEG <sub>2000</sub>	28	1.1	1 261	Aggregate NP	73	8805
NPr	PLA-PEG <sub>5000</sub>	13	-	201	Micelle	46	13 772

**Table VI** Maximum Drug Loading Calculated From the Structure and Affinity Parameters of Nanoparticles

Polymer Process	PLA-PEG <sub>2000</sub> Emulsion-evaporation	PLA-PEG <sub>5000</sub>	PLA-PEG <sub>2000</sub> Nanoprecipitation <sup>a</sup>	PLA-PEG <sub>5000</sub>
d <sub>H</sub> (nm)	126	141	54	27
K <sub>p</sub>	9578	8643	8805	13 772
M <sub>w</sub> <sup>NP</sup> × 10 <sup>-7</sup> (g/mol)	100	81.7	4.01	0.73
MaxLoading <sup>theo</sup> (w/w %) <sup>b</sup>	9.9	8.3	9.7	8.4

<sup>a</sup> For nanoprecipitation, C<sub>Acetone</sub><sup>PLA-PEG</sup> = 10 mg/mL

<sup>b</sup> Theoretical max loading was calculated from Eq. 19

between the cabazitaxel/nanoparticle interactions, evaluated from the K<sub>p</sub>, and the calculated packing of PLA-PEG chains, evaluated from V<sup>PLA-PEG</sup>, was put into evidence for both PLA-PEG copolymers (PLA-PEG<sub>2000</sub> or PLA-PEG<sub>5000</sub>) and both manufacturing processes (nanoprecipitation or emulsion-evaporation).

### Application of K<sub>p</sub> to Pharmaceutical Engineering

The partition coefficient, K<sub>p</sub> is related to the theoretical drug loading of nanoparticles by the equation:

$$\text{Drug loading} = \frac{m_{\text{encaps}}^{\text{drug}}}{(C_{\text{tot}}^{\text{drug}} + C_{\text{susp}}^{\text{PLA-PEG}}) V_{\text{ext}}} \sim \frac{K_p C_{\text{free}}^{\text{drug}} V_{\text{int}}}{C_{\text{susp}}^{\text{PLA-PEG}} V_{\text{ext}}} \quad (17)$$

In agreement with the experimental conditions, for which targeted drug loading was 5 w/w %, the approximation  $C_{\text{tot}}^{\text{drug}} V_{\text{ext}} \ll C_{\text{susp}}^{\text{PLA-PEG}} V_{\text{ext}}$  was used. According to the structure parameters of the nanoparticles (R<sub>H</sub> and M<sub>w</sub><sup>NP</sup>), determined above:

$$\text{Drug loading} \sim K_p C_{\text{free}}^{\text{drug}} \frac{4\pi R_H^3 N_A}{3M_w^{\text{NP}}} \quad (18)$$

Where N<sub>A</sub> is the Avogadro's number

Considering the Eq. 18, the maximal theoretical drug loading is reached when the concentration of free drug, C<sub>free</sub><sup>drug</sup>, is the highest. In order to avoid external crystallization of drug (Fig. 1), resulting in loss of drug and destabilization of the system, C<sub>free</sub><sup>drug</sup> should be lower than the maximal solubility of drug in the suspending media, i.e., water (S<sub>in water</sub><sup>drug</sup>) if the surfactant does not exhibit solubilizing properties. Thus, for one type of PLA-PEG nanoparticle and one specific drug, the theoretical maximal drug loading is expressed as:

$$\text{Maximal drug loading} \sim K_p S_{\text{in water}}^{\text{drug}} \frac{4\pi R_H^3 N_A}{3M_w^{\text{NP}}} \quad (19)$$

The maximal drug loading of cabazitaxel (S<sub>in water</sub><sup>cab</sup> = 8 µg/mL) was calculated for micelle and aggregated PLA-PEG

nanoparticles (Table VI). The values were not significantly different from each other and the mean maximal drug loading was 9.1 ± 0.9 w/w %. Interestingly, whatever the PLA-PEG copolymer (PLA-PEG<sub>2000</sub> or PLA-PEG<sub>5000</sub>) or the manufacturing process (nanoprecipitation or emulsion-evaporation) used, the encapsulation performance of the nanoparticles can be predicted.

The choice of one process or the other should be considered according to experimental facilities. The downside of nanoprecipitation, for the production of larger batches of nanoparticles is (i) the low concentration of the resulting suspension and (ii) the large quantity of solvent to be evaporated. Nevertheless, the nanoprecipitation process is very useful in a preformulation approach, as it requires a minimum amounts of drug substance and standard formulation equipment. At the same time, miniaturization of the emulsion-evaporation process, using sonication probe for example, can also be considered at the laboratory scale, before scale-up.

This methodological approach, only requiring simple determination of K<sub>p</sub> and the size of nanoparticle may be helpful to anticipate the aptness of hydrophobic drugs to be encapsulated in PLA-PEG nanoparticle. Moreover it may be less drug substance and time-consuming as compared to experimental design (37).

### CONCLUSION

The partition equilibrium of cabazitaxel between aqueous media and PLA-PEG nanoparticles manufactured by emulsion-evaporation and nanoprecipitation process was studied for PLA-PEG<sub>2000</sub> and PLA-PEG<sub>5000</sub>. The introduction of a solubilizing agent and its corresponding solubilization equilibrium gave access to the particle/water partition coefficient at zero concentration of solubilizing agent, which was shown to lead to the same value for HPβCD and BSA, as expected.

The drug/particle interaction, by mean of the partition coefficient K<sub>p</sub> was related to the structure of the nanoparticles. The nanoparticles made of both PLA-PEG<sub>2000</sub> and PLA-PEG<sub>5000</sub> structured as aggregates formed by the emulsion-evaporation as well as by the nanoprecipitation process, were characterized by the lower K<sub>p</sub> values. On the

opposite, the PLA-PEG<sub>5000</sub> micelles, nano-assembled by precipitation in specific conditions, were characterized by a higher  $K_p$  value and denser packing of the PLA-PEG chains (e.g., low  $V^{PLA-PEG}$ ). In an attempt to favor micelle formation over nanoparticles made of aggregates, by nanoprecipitation, the decrease of polymer concentration or the increase of surfactant concentration can be considered (38). More importantly, whatever the manufacturing process or the formulation conditions, it was shown that the drug/particle interaction can be related to the size and the aggregation number of the PLA-PEG nanoparticles.

From a process engineering standpoint, the maximal drug loading can be estimated from the  $K_p$  and information about the structure of nanoparticles in order to optimize the drug encapsulation yield during nanoparticle formation. Moreover  $K_p$  is useful to determine the free and encapsulated fractions of drug along the whole manufacturing process, and anticipate undesired release, in case of purification by extended dilutions or addition of cryoprotectants prone to solubilize the drug.

## ACKNOWLEDGMENTS AND DISCLOSURES

The post-doctorate fellowship of Odile Diou was financed by Sanofi. The authors would like to thank Guillaume Louit (Sanofi, Vitry sur Seine) for fruitful advices about partition experiments, Jean Alie (Sanofi, Montpellier) for TEM observations and Eric Didier (Sanofi, Vitry sur Seine) for synthesizing PLA-PEG copolymers. The authors acknowledge Thierry Verrecchia who did pioneering experiments on partition coefficient during his Pharm D thesis in 1998.

## REFERENCES

- Jain RK, Stylianopoulos T. Delivering nanomedicine to solid tumors. *Nat Rev Clin Oncol*. 2010;7:653–64.
- Prabhakar U, Maeda H, Jain RK. Challenges and key considerations of the enhanced permeability and retention effect for nanomedicine drug delivery in oncology. *Cancer Res*. 2013;73:2412–7.
- Yuan F, Dellian M, Fukumura D. Vascular permeability in a human tumor xenograft: molecular size dependence and cutoff size. *Cancer Res*. 1995;55:3752–6.
- Hrkach J, Von Hoff D, Mukkaram Ali M, Andrianova E, Auer J, Campbell T, et al. Preclinical development and clinical translation of a PSMA-targeted docetaxel nanoparticle with a differentiated pharmacological profile. *Sci Transl Med*. 2012;4:1–12.
- Bazile D, Verrecchia T, Bassoulet MT, Marlard M, Spenlehauer G, Veillard M. Ultradispersed polymer with rate and time control. *J Pharm Sci Technol Jpn*. 1993;53:10–3.
- Bazile D, Prud'homme C, Bassoulet MT, Marlard M, Spenlehauer G, Veillard M. Stealth Me.PEG-PLA nanoparticles avoid uptake by the mononuclear phagocytes system. *J Pharm Sci*. 1995;84:493–8.
- Bazile DV, Ropert C, Huve P, Verrecchia T, Mariard M, Frydman A, et al. Body distribution of fully biodegradable [14C]-poly(lactic acid) nanoparticles coated with albumin after parenteral administration to rats. *Biomaterials*. 1992;13:1093–102.
- Yamaoka T, Abataa AS, Ikada Y. Distribution and tissue uptake of Poly(ethylene glycol) with different molecular weights after intravenous administration to mice. *J Pharm Sci*. 1994;83:601–6.
- Qian H, Wohl AR, Crow JT, Macosko CW, Hoye TR. A strategy for control of “random” copolymerization of lactide and glycolide: application to synthesis of PEG-b-PLGA block polymers having narrow dispersity. *Macromolecules*. 2011;44:7132–40.
- Plard JP, Bazile D. Comparison of the safety profiles of PLA50 and Me.PEG-PLA50 nanoparticles after single dose intravenous administration to rat. *Colloids Surf B: Biointerfaces*. 1999;16:173–83.
- Riley T, Stolnik S, Heald CR, Xiong CD, Garnett MC, Illum L, et al. Physicochemical evaluation of nanoparticles assembled from Poly(lactic acid)-Poly(ethylene glycol) (PLA-PEG) block copolymers as drug delivery vehicles. *Langmuir*. 2001;17:3168–74.
- Torchilin V. Tumor delivery of macromolecular drugs based on the EPR effect. *Adv Drug Deliv Rev*. 2011;63:131–5.
- Acharya S, Sahoo SK. PLGA nanoparticles containing various anticancer agents and tumour delivery by EPR effect. *Adv Drug Deliv Rev*. 2011;63:170–83.
- Reddy LH, Bazile D. Drug delivery design for intravenous route with integrated physicochemistry, pharmacokinetics and pharmacodynamics: illustration with the case of taxane therapeutics. *Adv Drug Deliv Rev*. 2014;71:34–57.
- Stern ST, Hall JB, Yu LL, Wood LJ, Paciotti GF, Tamarkin L, et al. Translational considerations for cancer nanomedicine. *J Control Release*. 2010;146:164–74.
- Tyner K, Sadrieh N. Characterization of Nanoparticles Intended for Drug Delivery: S.E. McNeil; 2011.
- Delie F, Pascale Ribaux P, Petignat P, Cohen M. Anti-KDEL-coated nanoparticles: a promising tumor targeting approach for ovarian cancer? *Biochimie*. 2012;94:2391–7.
- Hu Q, Gu G, Liu Z, Jiang M, Kang T, Miao D, et al. F3 peptide-functionalized PEG-PLA nanoparticles co-administrated with tLyp-1 peptide for anti-glioma drug delivery. *Biomaterials*. 2013;34:1135–45.
- Verrecchia T. Mécanisme de libération *in vitro* d'une molécule hydrophobe encapsulée dans des nanoparticules d'un copolymère de poly(acide lactique) et de poly(éthylène glycol) PLA-PEG; 1998.
- Landry FB, Bazile DV, Spenlehauer G, Veillard M, Kreuter J. Release of the fluorescent marker Prodan from poly(D, L-lactic acid) nanoparticles coated with albumin or polyvinyl alcohol in model digestive fluids (USP XXII). *J Control Release*. 1997;44:227–36.
- Illum L, Khan MA, Mak E, Davis SS. Evaluation of carrier capacity and release characteristics for poly(butyl-2-cyanoacrylate) nanoparticles. *Int J Pharm*. 1986;30:17–28.
- Matsuoka K, Moroi Y. Micelle formation of sodium deoxycholate and sodium ursodeoxycholate (Part 1). *Biochim Biophys Acta*. 2002;1580:189–99.
- Mark JE. *Polymer data handbook*: Oxford university press; 1999.
- Vitale SA, Katz JL. Liquid droplet dispersions formed by homogeneous liquid-liquid nucleation: “The Ouzo Effect”. *Langmuir*. 2003;19:4105–10.
- Botet R. The “ouzo effect”, recent developments and application to therapeutic drug carrying. *Journal of Physics: Conference Series*. 2012; 352.
- Lepeltier E, Bourgaux C, Couvreur P. Nanoprecipitation and the “Ouzo effect”: application to drug delivery devices. *Adv Drug Deliv Rev*. 2014;71:86–97.
- Johnson BK, Prud'homme RK. Mechanism for rapid self-assembly of block copolymer nanoparticles. *Phys Rev Lett*. 2003;91:118302.
- Legrand P, Lesieur S, Bochet A, Gref R, Raatjes W, Barratt G, et al. Influence of polymer behaviour in organic solution on the

- production of polylactide nanoparticles by nanoprecipitation. *Int J Pharm.* 2007;344:33–43.
29. Gao Z, Varshney SE, Wong S, Eisenberg A. Block Copolymer “Crew-Cut” Micelles in water. *Macromolecules.* 1994;27:7923–7.
  30. Louguet S, Kumar AC, Guidolin N, Sigaud G, Duguet E, Lecommandoux S, *et al.* Control of the PEO chain conformation on nanoparticles by adsorption of PEO-block-Poly(L-lysine) copolymers and its significance on colloidal stability and protein repellency. *Langmuir.* 2011;27:12891–901.
  31. De Gennes PG. Conformations of polymers attached to an interface. *Macromolecules.* 1980;13:1069–75.
  32. De Gennes PG. Polymers at an interface—a simplified view. *Adv Colloid Interf Sci.* 1987;27:189–209.
  33. Karnik R, Gu F, Basto P, Cannizzaro C, Dean L, Kyei-Manu W, *et al.* Microfluidic platform for controlled synthesis of polymeric nanoparticles. *Nanoletters.* 2008;8:2906–12.
  34. Desgouilles S, Vauthier C, Bazile DV, Vacus J, Grossiord JL, Veillard M, *et al.* The design of nanoparticles obtained by solvent evaporation: a comprehensive study. *Langmuir.* 2003;19:9504–10.
  35. Rübe A, Hause G, Mäder K, Kohlbrecher J. Core-shell structure of Miglyol/poly(D, L-lactide)/Poloxamer nanocapsules studied by small-angle neutron scattering. *J Control Release.* 2005;107:244–52.
  36. Anderson KS, Hillmyer MA. Melt chain dimensions of polylactide. *Macromolecules.* 2004;37:1857–62.
  37. Julienne MC, Alonso MJ, Gomez Amoza JL, JPB. Preparation of Poly(D,L-Lactide/Glycolide) nanoparticles of controlled particle size distribution: application of experimental designs. *Drug Dev Ind Pharm.* 1992;18:1063–77.
  38. Stepanyan R, Lebouille JGJL, Slot JJM, Tuinier R, Cohen Stuart MA. Controlled nanoparticle formation by diffusion limited coalescence. *Phys Rev Lett.* 2012;109:138301.